ELSEVIER

Journal of Power Sources 105 (2002) 297–304

JOURNAL OF POWER SOURCES

www.elsevier.com/locate/jpowsour

Activity of $PtRuMeO_x$ (Me = W, Mo or V) catalysts towards methanol oxidation and their characterization

Z. Jusys[a,*], T.J. Schmidt[a,1], L. Dubau[a,2], K. Lasch[b], L. Jörissen[b], J. Garche[b], R.J. Behm[a]

[a]*Abteilung Oberflächenchemie und Katalyse, Universität Ulm, D-89069 Ulm, Germany*
[b]*Zentrum für Sonnenenergie- und Wasserstoff-Forschung, Helmholtzstraße 8, D-89081 Ulm, Germany*

Abstract

The activity of unsupported ternary $PtRuMeO_x$ (Me = W, Mo, V) high surface area catalysts towards methanol oxidation under fuel cell relevant conditions, at constant potential and elevated temperature of 60 °C, was investigated by the thin-film electrode method. CO-stripping experiments for actual surface area detection, using differential electrochemical mass spectrometry (DEMS) to evaluate the amount of adsorbed CO, show that the electrochemically active area of the particle surface is significantly smaller than the total particle surface area determined by N_2 BET measurements, indicating that part of their surface consists of MeO_x. The specific surface activity of the catalysts towards methanol oxidation at 60 °C, normalized to the current density per square centimeter of electrochemically active noble metal surface, decreases in the order $PtRuVO_x > PtRuMoO_x > PtRu > PtRuWO_x = PtRu$ (E-TEK). Apparently, the surface oxide leads to an acceleration of the methanol oxidation reaction, which is, however, partly compensated by a decrease in active surface area.

Keywords: Methanol; Electrooxidation; PtRu alloys; Ternary catalysts; Transition metal oxides; Active surface area; DEMS

1. Introduction

One of the major problems for the efficient conversion of methanol fuel to electric current in a direct methanol fuel cell (DMFC) is the slow methanol oxidation kinetics on the anode catalysts. This is mostly due to a self-poisoning of the surface by reaction intermediates such as CO, which are formed during stepwise dehydrogenation of methanol [1]. Therefore, in order to improve the efficiency of the DMFC, anode catalysts are required which combine a high activity for methanol dehydrogenation and an improved tolerance towards CO poisoning.

Pt, the standard catalyst for the oxidation of organic molecules including methanol [2–4], is rather active for the dehydrogenation step, but suffers from a high sensitivity towards CO poisoning. Therefore, methanol oxidation on Pt is only possible at potentials where adsorbed CO and other poisoning intermediates are effectively oxidized, leading to a significant overpotential and hence loss in efficiency. A higher efficiency at more negative potentials is obtained for PtRu catalysts, which is generally attributed to their superior CO tolerance due to a bifunctional effect, where CO is oxidized by OH species generated on Ru surface atoms [5]. However, the efficiency of the DMFCs operating on PtRu anode catalysts is still insufficient for practical applications. Further optimization of the anode material for the DMFC is thus important. Therefore, a number of other catalyst systems have been investigated for their suitability as methanol oxidation catalysts, including platinum alloy catalysts other than PtRu such as PtSn [6,7] or PtMo [8,9], ternary and higher PtRu-based alloy catalysts, such as PtRuOs [10], PtRuSn [11], PtRuW [12], PtRuSnW [13,14] or PtRuOsIr [15] (see also [16]). Another, slightly different approach involved the use of ternary $PtRuMeO_x$ (Me = W, Mo, V) catalysts, which were shown to have an enhanced catalytic activity towards methanol oxidation compared to PtRu catalysts [17]. These different classes are similar in so far as under reaction conditions the non-noble metals (and also Ru) as well as their respective oxides were shown to be active sites for the formation of oxy-species (see, e.g. [18]).

We here present results of a comparative study of the activity of ternary $PtRuMeO_x$ (Me = W, Mo, V) catalysts

* Corresponding author. Permanent address: Institute of Chemistry, A. Gostauto 9, 2600 Vilnius, Lithuania. Tel.: +370-2-611543; fax: +370-2-617018.
E-mail address: jusys@ktl.mii.lt (Z. Jusys).
[1] Present address: Lawrence Berkeley National Laboratory, Materials Science Division, Berkeley, CA 94720, USA.
[2] Present address: UMR-CNRS 6503, Université de Poitiers, F-86022 Poitiers, France.

0378-7753/02/$ – see front matter
PII: S0378-7753(01)00955-7

towards methanol oxidation under fuel cell relevant conditions, at constant electrode potential and elevated temperature of 60 °C. The potentiostatic methanol oxidation current, measured at fuel cell relevant temperatures [19] on the recently developed thin-film electrode [20], was taken as a simple electrochemical measure for the catalytic activity towards methanol oxidation under fuel cell relevant conditions. This way the mass specific currents (in mA mg^{-1} of the catalyst) or the current densities (in mA per geometric area) can be evaluated at constant electrode potentials. Both parameters are important in terms of practical applications. For assessing the catalytic activity of different high surface area catalysts, however, the measured currents should be normalized with respect to the electrochemically active surface area of the electrode [21]. The active surface area of the noble metal of the catalyst was evaluated via oxidation of pre-adsorbed, saturated CO adlayers (CO-stripping). In order to avoid contributions from charging of the double-layer to the faradaic charge during CO stripping, especially on PtRu, we monitored CO_2 formed by differential electrochemical mass spectrometry (DEMS) [22], using a thin-layer flow-through cell [23,24]. For comparison, the total surface area was determined by nitrogen adsorption BET measurements.

In the following, after a brief description of the experimental setup and procedures, we will first calibrate the DEMS setup for CO-stripping using a massive Pt electrode with defined surface area as the reference, then assess the active surface area of the unsupported high area $PtRuMeO_x$ and PtRu catalysts by CO-stripping, by comparison with the Pt electrode, and finally present and discuss the thin film electrode measurements on the methanol oxidation activity of these catalysts.

2. Experimental

2.1. Catalyst synthesis and characterization

The catalysts were prepared using a modified Adams method [25] as described in a previous paper [17]. Briefly, appropriate amounts of the noble metal halides and transition metal oxides were intimately mixed with an excess of sodium nitrate and the mixture was fused at 500 °C for 3 h. The residue was then washed thoroughly with water to remove nitrate and chloride ions, and the resulting aqueous suspension of mixed oxides was reduced at room temperature by hydrogen gas [17]. A commercial unsupported PtRu (E-TEK) was used to compare the performance of the catalysts.

The bulk composition of the catalysts was determined by energy dispersive X-ray emission (EDX), the values for the different catalysts (Pt:Ru ratio ∼ 50:50) are listed in Table 1. The particle size and the crystallinity of the catalyst powders were investigated by X-ray diffraction (XRD) (see [17] for the details). The geometric surface area of the catalyst was calculated from the BET measurements using nitrogen gas as adsorbate. Both methods led to mean particle sizes of 3–5 nm [17]. Estimates of the Ru metal content in the alloy particles, by comparison with the lattice constant of bulk alloys with different Pt:Ru compositions [26], are equally listed in Table 1. The values of between 2 and 18% Ru metal content are significantly lower than the nominal Ru bulk content, implying that the majority of the Ru is not included in the alloy, but rather present in an oxidic phase. Similar observations on carbon supported PtRu catalysts were reported recently [27]. Strictly speaking these results describe the situation before the electrocatalytic characterization only. We do not expect, however, the Ru oxides to be fully reduced under reaction conditions.

2.2. Working electrode preparation

The working electrodes for the electrochemical measurements were prepared using the recently developed thin-film electrode method [20]. In short, 20 μl of an aqueous catalyst suspension (0.5 mg ml^{-1}) was pipetted onto a mirror-finished glassy carbon substrate (Hochtemperatur Werkstoffe GmbH), yielding a total catalyst loading of 35 μg catalyst per square centimeter. After evaporating the water under a stream of argon, an aqueous Nafion® solution, prepared as described in [19], was successively pipetted onto the catalyst in order to fix the particles on the substrate. The Nafion® film resulting after evaporating the water had a thickness of about 0.2 μm, so that diffusion limitations caused by the film were negligible [20]. All measurements were carried out in 0.5 M H_2SO_4 (Merck suprapure). A saturated calomel electrode (SCE) was used as reference electrode. All potentials, however, are referred to that of the reversible hydrogen electrode (RHE) in the same electrolyte.

Table 1
Characterization of the high surface area catalysts

Catalyst	Bulk composition (EDX) (%)	Ru fraction in alloy particles (%)	BET surface area ($m^2\ g^{-1}$)	CO-stripping surface area ($m^2\ g^{-1}$)
Pt/Ru (E-TEK)	54% Pt; 46% Ru	10	126	66
Pt/Ru	55% Pt; 45% Ru	18	82	37
$Pt/Ru/Wo_x$ Pt:W (8:1)	54% Pt; 39% Ru; 7% W	2	120	15
$Pt/Ru/MoO_x$ Pt:Mo (7:1)	56% Pt; 36% Ru; 8% Mo	8	108	20
$Pt/Ru/VO_x$ Pt:V (7:1)	52% Pt; 40% Ru; 8% V	10	90	21

2.3. Oxidation of adsorbed CO monolayers (CO stripping)

The thin-film electrodes for DEMS measurements were prepared on glassy carbon disks (diameter 9 mm) in the same way as described above. The diameter of the catalyst circle centered on the glassy carbon surface was, however, only ca. 6 mm. The electrode was mounted into a thin-layer flow-through DEMS cell following the design described in [23,24], so that the catalyst was exposed to the solution through a centered circular spacer (i.d. 6 mm) of ca. 100 μm thickness. The gaseous products were evaporated into the mass spectrometer through a bare porous membrane (Scimat®, 60 μm thick, 50% porosity, 0.2 μm pore diameter). A smooth polycrystalline Pt (Matek, 9 mm in diameter) with an exposed area 0.28 cm^2 was used for the reference experiments described below.

The electrolyte flow through the DEMS cell (5 μl s^{-1}) was ensured by the hydrostatic pressure in the supply bottle filled with electrolyte, which was constantly purged by argon (MTI Gase, N6.0). CO (Messer–Griesheim N4.7) was adsorbed at a constant electrode potential of 0.11 V. CO-saturated electrolyte was inserted with a syringe of 2 ml volume through a separate inlet. Afterwards, the thin-layer cell was carefully washed with pure 0.5 M sulfuric acid and the CO-stripping experiments were performed ($v = 10$ mV s^{-1}).

The DEMS set-up was based on a Balzers QMS 112 quadrupole mass spectrometer, a Pine Instruments potentiostat and a computerized data acquisition system. Two Pt wires in the thin-layer cell served as counter electrodes. The reference electrode was connected to the DEMS cell at the outlet through the Teflon capillary.

2.4. Continuous methanol oxidation

Methanol electro-oxidation experiments were performed potentiostatically on stationary electrodes at 60 °C, reading the stabilized current values after 30 min of oxidation [19]. The thin-film electrodes based on glassy carbon support (6 mm in diameter, area 0.283 cm^2) were prepared as described in Section 2.3. The electrolyte was 0.5 M sulfuric acid containing 1 M methanol (Merck, pro analysi) continuously purged with Ar. The reference electrode was connected to the main compartment of the cell through a closed electrolyte bridge.

3. Results and discussion

3.1. Evaluation of the active surface area

3.1.1. Adsorbed CO monolayer oxidation on a smooth polycrystalline Pt electrode

Initially, we calibrated the DEMS set-up versus pre-adsorbed CO-stripping and hydrogen adsorption using a massive polycrystalline Pt electrode. DEMS data for adsorbed CO-stripping from this smooth polycrystalline Pt electrode are shown in Fig. 1. Due to the strong adsorption of CO on Pt surfaces, hydrogen adsorption/desorption on Pt is completely blocked in the potential range of H_{upd}, between 0.02 and 0.35 V, indicating the presence of a saturated CO adlayer (Fig. 1a). At potentials anodic of the suppressed H_{upd}-region ($E > 0.3$ V), oxidation of weakly adsorbed CO occurs between 0.4 and 0.6 V, in the so-called pre-wave, followed by the main CO-stripping peak centered at $E = 0.7$ V (Fig. 1a). For details about the nature of the pre-wave CO oxidation, we refer to [28].

In the subsequent cathodic and anodic sweep, the base voltammogram (Fig. 1a) traces the current–potential pattern well-known for polycrystalline Pt from [2–4], demonstrating that the set-up and sample preparation resulted in well defined, clean electrode surfaces. Furthermore, from the charge below the desorption peak (54 ± 1 μC) and the geometric surface area of the electrode (0.28 cm^2) the roughness factor, RF, of the sample was determined to be $RF = 1.2 \pm 0.1$, assuming an adsorption charge of 210 μC cm^{-2} for a full H_{upd} monolayer [29] and a hydrogen coverage at the onset of H_2 evolution of $\theta_H = 0.77$ [30].

The Faradaic charge for CO-stripping, found by integrating the current in the potential range from 0.3 to 0.9 V after 10% correction due to the double-layer charging [24], is 96 μC. Considering the roughness factor determined by hydrogen UPD, the CO coverage on the polycrystalline Pt surface (Θ_{CO}) can be determined to be $\Theta_{CO} = 0.68$. The latter value is in a good agreement with literature data for the saturated CO adlayer coverage on Pt (1 1 1) single crystal surfaces ([28] and references cited therein).

The corresponding mass spectrometric cyclic voltammogram (MSCV) of the ion current $m/z = 44$ (CO_2^+ ion intensity), recorded simultaneously with the CV in Fig. 1a, is shown in Fig. 1b. As already mentioned, the MSCV in Fig. 1b is free from other (Faradaic or capacitive) contributions, which are present in the CV (hydrogen and oxygen adsorption/desorption, double-layer charging), since only the CO-stripping product (CO_2) is monitored by the mass spectrometer. The MSCV (Fig. 1b) nicely follows the Faradaic CO-stripping current (Fig. 1a). The slight shift of the MSCV peak to more positive potentials (10–20 mV) reflects the time required for the gaseous species formed at the electrode to reach the porous membrane and to diffuse into the mass spectrometer—the time constant of the thin-layer flow-through cell is 1–2 s in accordance with previous data [23]. The good signal-to-noise ratio of the MSCV (e.g. the pre-wave of CO oxidation is clearly resolved) demonstrates a good performance, in particular, a sufficient sensitivity (in the sub-monolayer range) of the DEMS system.

Integration of the mass spectrometric current above the ground level of the $m/z = 44$ signal gives a mass spectrometric charge of 1.65 nC. This charge corresponds to the real surface area of the Pt electrode of 0.33 cm^2. The ratio of the mass spectrometric charge to the real surface area for the smooth polycrystalline electrode will be used (Section 3.1.2)

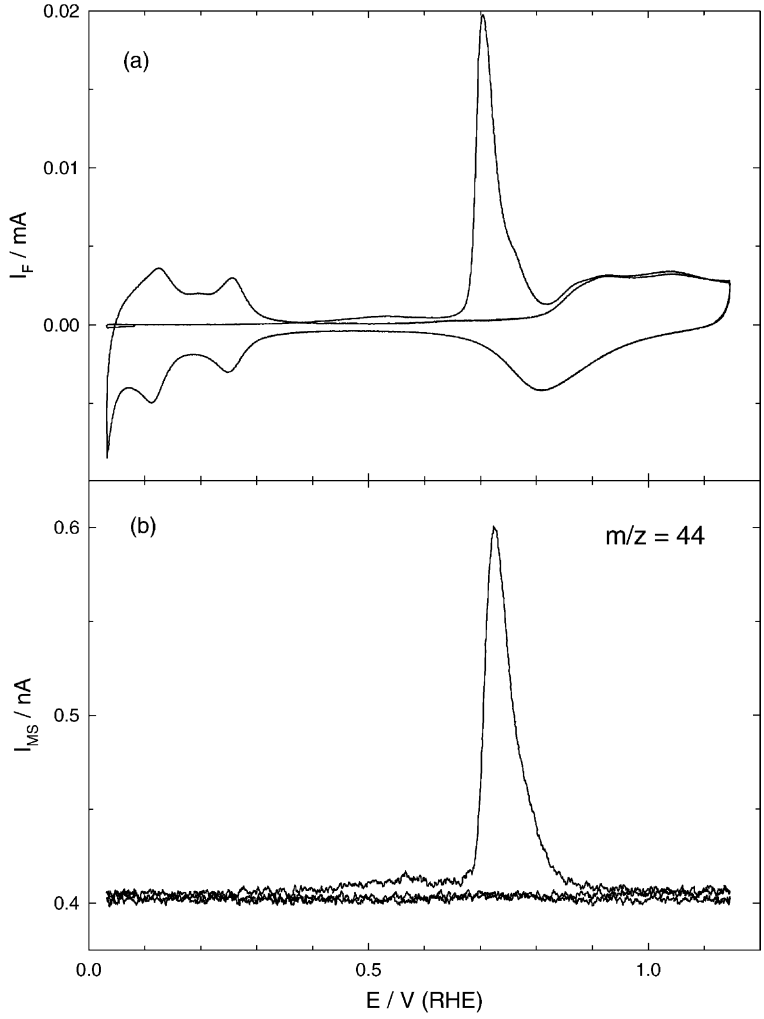

Fig. 1. (a) CV, and (b) MSCV, for adsorbed CO monolayer oxidation on a smooth polycry stalline Pt electrode in a thin-layer DEMS cell (0.5 M H_2SO_4, temperature 25 °C, potential scan rate 10 mV s^{-1}, electrolyte flow rate 5 μl s^{-1}).

as the standard for evaluation the active metal surface area of the high surface area electrodes. The sensitivity factor K^* [22], which relates the mass spectrometric signal to the Faradaic current for CO_{ad} oxidation, can be calculated from the DEMS data of Fig. 1. The ratio between the mass spectrometric charge multiplied by two (the number of electrons in CO oxidation reaction to CO_2) and the Faradaic charge is $K^* = 2 \times Q_{MS}/Q_F = 2 \times 1.65 \times 10^{-9}/0.096 \times 10^{-3} = 3.4 \times 10^{-5}$.

3.1.2. Adsorbed CO monolayer oxidation on high surface area electrodes

Similar measurements were performed for unsupported high surface area PtRu catalysts. Fig. 2 shows the resulting CO-stripping curves for a commercial, unsupported PtRu catalyst (E-TEK). Again, hydrogen adsorption/oxidation is completely suppressed after CO adsorption on the PtRu catalysts, suggesting the PtRu particles are covered by a saturated CO adlayer (Fig. 2a, solid line). Oxidation peak of pre-adsorbed CO occurs in the positive-going potential scan at about 0.5 V, which is 0.2 V negative as compared to Pt (Fig. 1a), in agreement with data [31–35]. After stripping the adsorbed CO the CV shows the typical behavior of a PtRu electrode (Fig. 2a, solid line). The Faradaic charge of CO-stripping found by integrating the current in the potential range from 0.06 to 0.86 V is 3.82 mC. It should be noted that the charge obtained by integrating the Faradaic current involves a large and undefined capacitive contribution due to the large double-layer current interfering with the CO-stripping charge.

This problem is avoided in DEMS experiment, since the MSCV of $m/z = 44$ (Fig. 2b) is free from capacitive effects. The signal intensity above the background signal of $m/z = 44$, which is entirely due to adsorbed CO oxidative stripping from the high surface area PtRu catalyst, yields an integrated mass spectrometric charge 32.8 nC. Using the sensitivity factor K^* determined above and normalizing to the mass spectrometric charge obtained from the smooth Pt sample, the mass spectrometric charge can be converted into the Faradaic charge, Q_F, for CO-stripping, yielding a value

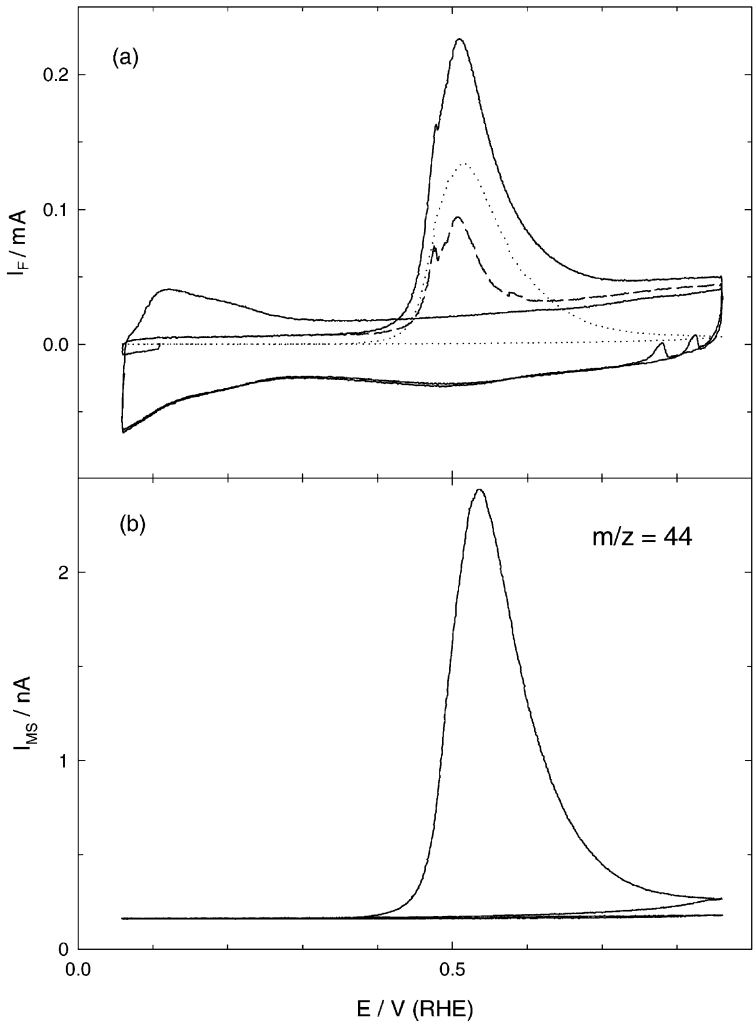

Fig. 2. CV (a, solid line) and MSCV (b) for adsorbed CO monolayer oxidation on an unsupported PtRu catalyst (E-TEK) in a thin-layer DEMS cell. Dotted and dashed line in (a) indicate the current density for CO_{ad} oxidation calculated from the MSCV (b) and the current for double-layer charging derived from the difference between the measured faradaic current and the CO_{ad} oxidation current found from the MSCV in (b), respectively (0.5 M H_2SO_4, temperature 25 °C, potential scan rate 10 mV s^{-1}, electrolyte flow rate 5 μl s^{-1}, catalyst loading 35 μg cm^{-2}).

of $Q_F = 1.9$ mC. This is about 50% of the total charge found by integrating the Faradaic current (Fig. 2a, solid line). A similar result was obtained recently for CO-stripping from electrodeposited PtRu alloy using DEMS [23]. The Faradaic CO-stripping current determined from the MSCV signal (corrected for the delay due to the time constant and the background $m/z = 44$ intensity) is included as dotted line in Fig. 2a. The double-layer charging partial current (Fig. 2a, dashed line) can be extracted from the DEMS data as the difference between the measured net current (Fig. 2a, solid line) and that calculated from the MSCV (Fig. 2a, dotted line).

The electrochemically active surface area of the catalysts, S_{act}, was evaluated from the DEMS data assuming that the coverage of the saturated CO adlayer on the metallic parts of the PtRu catalysts is the same as that on smooth polycrystalline Pt. It is calculated from the mass spectrometric charge obtained by integrating the MSCV (32.8 nC) and normalizing to the mass spectrometric charge obtained from the smooth Pt electrode (1.65 nC, 0.33 cm^2). This leads to an active surface area of the PtRu (E-TEK) catalyst of $S_{act} = 32.8 \times 0.33/1.65 = 6.6 \pm 0.1$ cm^2 (Fig. 2). Hence, the roughness factor RF for the PtRu (E-TEK) catalyst, defined as the ratio between the active and geometric surface area is $RF = 6.6/0.28 \approx 27$. At an absolute catalyst loading of 10 μg (35 μg cm^2), which includes any Ru present in an oxidic form (see [2].), this corresponds to a surface area of 66 ± 1 m^2 g^{-1} of the unsupported PtRu (E-TEK) catalyst.

Analogous DEMS measurements were carried out on the ternary $PtRuMeO_x$ catalysts synthesized by the Adams method. The results are shown in Table 1. For comparison, we also included the total surface area of these catalysts determined by BET measurements using nitrogen adsorption. Obviously, the electrochemically active area of the particle surface is different from the total particle surface area as calculated, e.g. from the metal loading and the dispersion or from the BET measurements. It was up to five times lower than the surface area found in the N_2 BET

measurements (Table 1). This result can be rationalized assuming that: (i) part of the metal particle surface is covered by MeO_x and/or that (ii) the actual metal content in the catalyst is lower than the nominal value due to the fact that part of the Ru is present in an oxidic form (see [27]). Both effects lead to a reduction of the accessible chemically active noble metal, since adsorption of CO takes place exclusively on oxide-free noble metal surface sites. A similar reduction in active surface is observed for the bimetallic PtRu catalyst, confirming the XRD result that it contains an appreciable amount of oxidic Ru per species under these conditions.

3.2. Continuous methanol oxidation on high surface area catalysts

After having characterized the different high area PtRu and $PtRuMeO_x$ catalysts by CO-stripping, we now focus on their activity for the continuous oxidation of methanol at constant potential. For this purpose, we performed potentiostatic measurements on these catalysts in 0.5 M sulfuric acid solution containing 1 M methanol at 60 °C. In contrast to dynamic methods such as cyclic voltammetry these potentiostatic measurements at elevated temperatures allow the catalyst activity to be studied under 'long-term' fuel cell relevant conditions, which is especially important when studying such self-poisoning reactions as methanol oxidation. The resulting potentiostatic current densities are shown in Fig. 3.

In Fig. 3a, we compared the mass specific current densities obtained for the ternary $PtRuMeO_x$ catalysts, an unsupported PtRu catalyst equally prepared by the Adams method and a commercial unsupported PtRu (E-TEK) catalyst. It should be noted that the exact stoichiometry of the catalysts, mainly the oxygen content in the ternary $PtRuMeO_x$ catalysts, is not known, which can lead to weight variations for similar metal contents. The resulting error in mass specific currents, due to an undefined amount of oxygen, can stem from two sources: (i) the unknown stoichiometry of the MeO_x; and (ii) the fraction of Ru present in oxidic form. While the former can be estimated to contribute less than 2% to the measured current, the latter contribution can be more significant, up to 7%.

Comparing the performance of the different catalysts in terms of mass specific current densities, without considering the presence of oxidic Ru species, the activity of the ternary $PtRuVO_x$ catalyst towards methanol oxidation is similar to that of the (unsupported) PtRu (E-TEK) catalyst. Both in turn are comparable to literature data for PtRu catalysts supported on Vulcan XC 72 carbon (E-TEK) [19]. Including the other unsupported $PtRuMeO_x$ catalysts the catalytic activity for continuous methanol oxidation at 60 °C in terms of the mass specific currents decreases in the order $PtRu(E\text{-}TEK) = PtRuVO_x > PtRu > PtRuMoO_x > PtRuWO_x$ (Fig. 3a).

As already mentioned in the introduction, the mass specific current density is a good measure for the catalytic activity from a practical point of view. From a more basic, chemical point of view, however, a better measure is the specific current density normalized to the active surface area, which includes the effects of varying particle sizes. This is even more important when comparing the activity of complex catalyst systems such as the present (ternary) $PtRuMeO_x$ and PtRu high surface area catalysts, where the electrochemically active noble metal surface area is decreased due to the presence of MeO_x on the ternary catalyst particle surface and due to the formation of oxidic Ru species.

The measured methanol oxidation currents replotted versus the electrochemically active surface area as determined from the CO-stripping DEMS experiments (Section 3.1.2) are shown in Fig. 3b. The specific surface activity of the catalysts towards methanol oxidation at 60 °C, normalized to the current density per 1 cm^2 noble metal surface area, decreases in the following sequence: $PtRuVO_x > PtRuMoO_x > PtRu > PtRuWO_x = PtRu$ (E-TEK). Hence, the specific current densities in Fig. 3b behave clearly

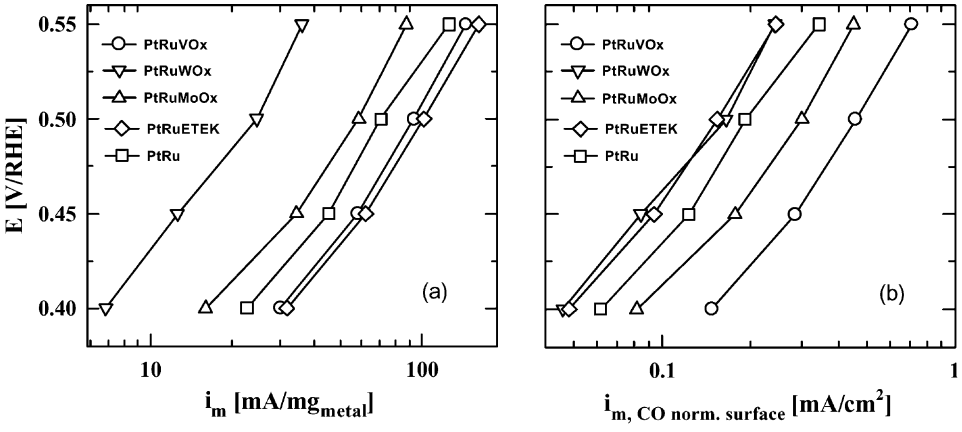

Fig. 3. Potentiostatic (30 min/potential) continuous methanol oxidation on high surface area catalysts: mass specific current densities (a) and specific current densities normalized to the active surface area (b) on unsupported $PtRuMeO_x$ and PtRu catalysts (0.5 M H_2SO_4 + 1 M CH_3OH, temperature 60 °C, catalyst loading 35 μg cm^{-2}).

different as compared to the mass specific current densities in Fig. 3a. Here, the ternary $PtRuVO_x$ catalyst shows the highest activity towards methanol oxidation among the catalysts studied (Fig. 3b). However, in terms of mass specific currents the activity of $PtRuVO_x$ catalyst is just similar to that of commercial PtRu (E-TEK) catalyst (Fig. 3a). Other catalysts synthesized by the Adams method exhibit even lower catalytic activities compared to commercial PtRu (E-TEK) in terms of mass specific currents (Fig. 3a), though most of them (except $PtRuWO_x$) show an enhanced activity compared to PtRu (E-TEK) catalyst in terms of specific current densities normalized versus the active surface area (Fig. 3b).

For catalyst particles of the same size and (nominal) Pt/Ru contents differences in the catalytic performance towards methanol oxidation, normalized versus the active noble metal surface area, can result from the following, partly counteracting effects: first, the transition metal oxides can improve the catalytic performance of the PtRu alloy surface, possibly by an enhanced oxidation of poisoning CO intermediates at the MeO_x/PtRu boundary. The oxidic species are not covered by CO and, due to their redox activity (multiple oxidation states), are effective for generating oxygen species from adsorbed water. These in turn can react with CO adsorbed on adjacent metallic sites. This mechanism closely resembles the bifunctional mechanism proposed for methanol and CO oxidation on PtRu, where Ru surface atoms are expected to act in a similar way [5]. Similar effects were proposed also for (hydrous) Ru oxides present on unsupported, binary PtRu catalysts [27]. Based on our XRD results the latter species are likely to contribute also in our measurements. On the other hand, the presence of MeO_x or RuO_x species on the catalyst particle surface decreases the active surface area of the noble metal particles as evidenced from the CO-stripping data (Table 1). As a result part of the noble metal becomes inactive due to the blocking of the PtRu surface by the oxidic species, which counteracts the above reaction enhancement. Furthermore, the interface between active metal and surface oxide may also affect the dehydrogenation of methanol, in addition to enhancing the removal of poisoning intermediates. It had been shown recently, for instance, that despite their improved CO oxidation activity PtSn catalysts are not more active for methanol oxidation as compared to Pt or even PtRu catalysts, demonstrating that an improved CO oxidation activity is not necessarily coupled to a better methanol oxidation performance [7,36]. Finally, the methanol oxidation activity is known to be sensitive to the Pt:Ru surface ratio [21,37]), which will vary significantly based on the pronounced differences in metallic Ru content in the particles determined by XRD.

While there is no doubt that these effects will contribute to the methanol oxidation activity of the ternary $PtRuMeO_x$ catalysts, a quantification of the individual contributions is not possible from the present data. Further electrochemical and in situ spectroscopic measurements are required to elucidate these effects and in particular the role of the surface oxide species. This also includes varying the amount (concentration) of the surface oxide species. The mechanistic insights are the basis for a further directed optimization of this interesting class of catalysts.

4. Summary

Using potentiostatic measurements on thin film electrodes we determined the catalytic activity of unsupported, high area ternary $PtRuMeO_x$ (Me = W, Mo, V) catalysts and, for comparison, of unsupported PtRu catalysts, for the continuous oxidation of methanol under fuel cell relevant conditions, i.e. at constant potential and elevated temperatures (60 °C). As a measure of the catalytic activity we used the specific current density normalized to the electrochemically active surface area of the active metal. The latter was determined by CO-stripping using on-line mass spectrometry (DEMS) for detection of the CO_2 formed, and a massive polycrystalline Pt electrode for reference. The specific surface activity of the catalysts towards methanol oxidation at 60 °C, normalized to the current density per square centimeter of noble metal surface area, decreases in the order $PtRuVO_x > PtRuMoO_x > PtRu > PtRuWO_x =$ PtRu (E-TEK).

Acknowledgements

We gratefully acknowledge financial support by the Federal Ministry for Education, Science, Research and Technology (BMBF) via Grant No. 3330341 and a fellowship by the DAAD for one of us (LD).

References

[1] T.D. Jarvi, E.M. Stuve, in: J. Lipkowsi, P.N. Ross (Eds.) Electrocatalysis, Wiley, New York, 1998, p. 75.
[2] W. Vielstich, Fuel Cells, Wiley/Interscience, London, 1970.
[3] R. Parsons, T. VanderNoot, J. Electroanal. Chem. 257 (1988) 257.
[4] B. Beden, J.M. Leger, C. Lamy, in: J.O'M. Bockris, B.E. Conway, R.E. White (Eds.), Modern Aspects of Electrochemistry, Vol. 22, Plenum Press, New York, 1992, p. 97.
[5] M. Watanabe, S. Motoo, J. Electroanal. Chem. 60 (1975) 267.
[6] A.N. Haner, P.N. Ross, J. Phys. Chem. 95 (1991) 3740.
[7] K. Wang, H.A. Gasteiger, N.M. Markovic, P.N. Ross, Electrochim. Acta 41 (1996) 2587.
[8] M. Götz, H. Wendt, Electrochim. Acta 43 (1998) 3637.
[9] J. Wang, H. Nakajima, H. Kita, Electrochim. Acta 35 (1990) 232.
[10] K.L. Ley, R. Liu, C. Pu, Q. Fan, N. Leyarovska, C. Segre, E.S. Smotkin, J. Electrochem. Soc. 144 (1997) 1543.
[11] A. Aramata, M. Masuda, J. Electrochem. Soc. 138 (1991) 1949.
[12] C. He, H.R. Kunz, J.M. Fenton, J. Electrochem. Soc. 144 (1997) 970.
[13] A.S. Aricò, Z. Poltarzewski, H. Kim, A. Morana, N. Giordano, V. Antonucci, J. Power Sour. 55 (1995) 159.
[14] A.S. Aricò, P. Creti, N. Giordano, V. Antonucci, P.L. Antonucci, A. Chuvilin, J. Appl. Electrochem. 26 (1996) 959.

[15] E. Reddington, A. Sapienza, B. Gurrau, R. Viswanathanm, S. Sarangapani, E.S. Smotkin, T.E. Mallouk, Science 280 (1998) 1735.
[16] M. Götz, H. Wendt, Electrochim. Acta 43 (1998) 3637.
[17] K. Lasch, L. Jörissen, J. Garche, J. Power Sour. 84 (1999) 225.
[18] S. Mukerjee, J. McBreen, J. Electrochem. Soc. 146 (1999) 600.
[19] T.J. Schmidt, H.A. Gasteiger, R.J. Behm, Electrochem. Commun. 1 (1999) 1.
[20] T.J. Schmidt, H.A. Gasteiger, G.D. Stäb, P.M. Urban, D.M. Kolb, R.J. Behm, J. Electrochem. Soc. 145 (1998) 2354.
[21] J.P. Iudice de Souza, T. Iwasita, F.C. Nart, W. Vielstich, J. Appl. Electrochem. 30 (2000) 43.
[22] O. Wolter, J. Heitbaum, Ber. Bunsenges. Phys. Chem. 88 (1984) 2.
[23] Z. Jusys, H. Massong, H. Baltruschat, J. Electrochem. Soc. 146 (1999) 1093.
[24] H. Baltruschat, in: A. Wieckowski (Ed.), Interfacial Electrochemistry: Theory, Experiment, Applications, Marcel Dekker, New York, 1999, p. 577.
[25] R. Adams, R.L. Schriner, J. Am. Chem. Soc. 45 (1923) 2171.
[26] H.A. Gasteiger, P.N. Ross Jr., E.J. Cairns, Surf. Sci. 293 (1993) 67.
[27] D. Rolison, P.L. Hagans, K.E. Swider, J.W. Long, Langmuir 15 (1999) 774.
[28] N.M. Markovic, B.N. Grgur, C.A. Lucas, P.N. Ross, J. Phys. Chem. B 103 (1999) 487.
[29] V.S. Bagotzky, Y.B. Vassilyev, Electrochim. Acta 12 (1967) 1323.
[30] T. Biegler, D.A. Rand, R. Woods, J. Electroanal. Chem. 29 (1971) 269.
[31] P.N. Ross Jr., in: J. Lipkowski, P.N. Ross (Eds.), Electrocatalysis, Wiley, New York, 1998, p. 43.
[32] H. Gasteiger, N. Markovic, P.N. Ross Jr., E.J. Cairns, J. Phys. Chem. 97 (1993) 12020.
[33] H. Gasteiger, N. Markovic, P.N. Ross Jr., E.J. Cairns, J. Phys. Chem. 98 (1994) 617.
[34] M. Krausa, W. Vielstich, J. Electroanal. Chem. 379 (1994) 307.
[35] R. Ianniello, V.M. Schmidt, U. Stimming, J. Stumper, A. Wallau, Electrochim. Acta 39 (1994) 1836.
[36] T.J. Schmidt, H.A Gasteiger, R.J. Behm, in: J. Russow, G. Sandstede, R. Staab (Eds.), Elektrochemische Reaktionstechnik und Synthese—Von den Grundlagen bis zur industriellen Anwendung, GDCH Monographie, Vol. 14, Gesellschaft Deutscher Chemiker, Frankfurt, 1999, p. 196.
[37] H.A. Gasteiger, N. Markovic, P.N. Ross, E.J. Cairns, J. Electrochem. Soc. 141 (1994) 1795.